

PREPARED FOR SUBMISSION TO JCAP

Photon horizon including Lorentz Invariance Violation.

Rodrigo Guedes Lang^a Humberto Martínez-Huerta^b Vitor de Souza^a

^aInstituto de Física de São Carlos, Universidade de São Paulo,
Av. Trabalhador São-carlense 400, São Carlos, Brasil.

^bDepartamento de Física, Centro de Investigación y de Estudios Avanzados del I.P.N.,
Apartado Postal 14-740, 07000, Ciudad de México, México.

E-mail: rodrigo.lang@usp.br, hmartinez@fis.cinvestav.mx, vitor@ifsc.usp.br

Abstract. In this paper, Lorentz Invariance Violation (LIV) is considered in the calculations of photon propagation in the Universe. LIV is considered only in the photon sector and the mean free path of the $\gamma\gamma \rightarrow e^+e^-$ interaction is calculated. The corresponding photon horizon including LIV effects is used to predict major changes in the propagation of photons with energy above 10^{16} eV. The GZK photon flux on Earth is calculated and compared to the Lorentz invariant scenario. It is shown that upper limits on the photon flux at the highest energies can set limits on the LIV coefficients.

Contents

1	Introduction	1
2	Description of the LIV model	2
3	Photon horizon including LIV effects	3
4	GZK photons including LIV effects	5
5	Conclusions	5

1 Introduction

Astroparticle physics has recently reached the status of precision science due to: a) the construction of new observatories operating innovative technologies, b) the detection of large numbers of events and sources and c) the development of clever theoretical interpretations of the data. Two observational windows have produced very important results in the last decade. The ultra-high energy cosmic rays ($E > \text{EeV}$) studied by the Pierre Auger and the Telescope Array Observatories [8, 34] improved our knowledge of the most extreme phenomena known in Nature. The GeV-TeV gamma-ray experiments FERMI/LAT [3], H.E.S.S. [28], MAGIC [29] and VERITAS [27] gave a new perspective on gamma-ray production and propagation in the Universe. The operation of the current instruments and the construction of future ones [9, 19] guarantee the production of even more precise information in the decades to come.

Lorentz Invariance (LI) is one the pillars of modern physics and it has been tested in several experimental approaches [26]. Astroparticle physics has been proposed as an appropriate test environment for possible Lorentz Invariance Violation (LIV) given the large energy of the particles, the large propagation distances, the accumulation of small interaction effects and recently the precision of the measurements [2, 12, 13, 20, 23, 32, 33].

Gamma-ray propagation in the intergalactic photon background was studied previously in detail [10]. In the present work, LIV is allowed in the interaction of high energy photons with the background and its consequences are studied. The LIV framework is explained in section 2. Only the $\gamma\gamma \rightarrow e^+e^-$ interaction is considered to violate Lorentz Invariance. The broken symmetry leads to a change of the energy threshold of the interaction. The allowed kinematic solutions for the interaction under a given LIV model are presented and discussed.

The effect of the change in the energy threshold modifies the mean free path of the interaction and therefore the survival probability of a photon propagating in the background depends on the LIV coefficients. This dependence is calculated in section 3 in which the mean free path and the survival probability are shown for several LIV coefficients and expansion orders of the energy dispersion relation.

Finally the mean free path of the $\gamma\gamma$ interaction considering LIV is implemented in a Monte Carlo propagation code. The effect of LIV in the flux of ultra high energy photons arriving on Earth due to the GZK effect is calculated. This result can be directly compared to measurements of upper limits on the flux of photons done by ultra high energy cosmic ray (UHECR) experiments in order to set limits on the LIV coefficients.

2 Description of the LIV model

One of the most commonly mechanisms to introduce LIV in particle physics phenomenology is based on the polynomial correction in the dispersion particle relation, mainly motivated by an extra term in the Lagrangian density that explicitly breaks Lorentz symmetry, see for instance references [2, 6, 12, 13, 20, 22, 24]. In these models, the corrected expression for the dispersion relation is given by the following equation:

$$E^2 - p^2 = m^2 + \delta_n E^{n+2}, \quad (2.1)$$

where (E, p) stands for the particle four-momenta with mass m . For simplicity, natural units are used in this section. δ_n is the LIV coefficient that parametrizes the particle dependent LIV correction and n expresses the correction order. The correction order can be derived from the series expansion or from a particular model for that order, see for instance the case of $n = 0$ [21], $n = 1$ [30] or for a generic n [35]. δ_n is frequently considered to be inversely proportional to E_{QG}^n [1, 2, 11, 24, 35, 37].

Equation 2.1 leads to unconventional solutions of the energy threshold in particle production processes of the type $AB \rightarrow CD$. In this paper, the $\gamma\gamma_{CB} \rightarrow e^+e^-$ interaction will be considered. From now on, the symbol γ refers to a high energy gamma ray with energy $E_\gamma = [10^9, 10^{22}]$ eV traveling in the Universe and interacting with the background photons named γ_{CB} with energy $\epsilon = [10^{-11}, 10]$ eV.

Considering LIV only in the photon sector, the specific dispersion relation can be written:

$$\begin{aligned} E_\gamma^2 - p_\gamma^2 &= \delta_{\gamma,n} E_\gamma^{n+2}, \\ \epsilon^2 - p_{\gamma_{CB}}^2 &= \delta_{\gamma,n} \epsilon^{n+2}, \end{aligned} \quad (2.2)$$

where $\delta_{\gamma,n}$ is the n -order LIV coefficient in the photon sector and therefore taken to be the same in both dispersion relations. The standard LI dispersion relation for the electron-positron pair follows: $E_{e^\pm}^2 - p_{e^\pm}^2 = m_e^2$.

Taking into account the inelasticity (K) of the process ($E_{e^-} = KE_\gamma$) and imposing energy-momentum conservation in the interaction, the following expression for a head-on collision with collinear final momenta can be written to leading order in $\delta_{\gamma,n}$

$$\begin{aligned} 4\epsilon E_\gamma - m_e^2 \left(\frac{1}{K(1-K)} - \frac{m_e^2}{2K(1-K)(E_\gamma + \epsilon)^2} \right) \\ = -\delta_{\gamma,n} E_\gamma^{n+2} \left[1 + \frac{\epsilon^{n+2}}{E_\gamma^{n+2}} - \frac{\epsilon}{E_\gamma} \left(1 + \frac{\epsilon^n}{E_\gamma^n} \right) \right]. \end{aligned} \quad (2.3)$$

In the ultra relativistic limit $E_\gamma \gg m_e$ and $E_\gamma \gg \epsilon$, this equation reduces to

$$\delta_{\gamma,n} E_\gamma^{n+2} + 4E_\gamma \epsilon - m_e^2 \frac{1}{K(1-K)} = 0. \quad (2.4)$$

Equation 2.4 implies two scenarios: I) $\delta_{\gamma,n} > 0$ the photo production threshold energy is shifted to lower energies and II) $\delta_{\gamma,n} < 0$ the threshold takes place at higher energies than that expected in a LI regime, except for scenarios below a critical value for delta where the photo production process is forbidden. Figure 1 shows the solution of equation 2.4 in an innovative way for $n = 0$. The inelasticity is fixed to $K = 1/2$. Three panels are shown: the left panel corresponds to $\delta_{\gamma,0} < 0$, the center panel corresponds to the LI solution with

$\delta_{\gamma,0} = 0$ and the right panel to the solution with $\delta_{\gamma,0} > 0$. The gray areas show the allowed regions of E_γ as a function of $\delta_{\gamma,0}$. The boundary of the shaded areas represents the allowed solutions of equation 2.4 when the background photon energy is equal to 2.7, 2, 1.5 and 1 K, from darker to lighter gray, respectively. The allowed regions are cumulative, the allowed area for 1 K includes higher temperatures. The red dashed line is the solution of equation 2.4 for $\delta_{\gamma,0} = 0$ (LI case) and $T = 2.7$ K. The red dashed line is shown in the left and right panels as a reference. Similar figures were produced for $n = 1, 2$, resulting in the same conclusions. In this work, the effects for $\delta_{\gamma,n} > 0$ are negligible when compared to $\delta_{\gamma,n} < 0$, therefore only the negative case will be discussed in the next sections.

Notice that, if $\delta_{\gamma,n} = 0$ in equation 2.4 the LI regime is recovered. In the LI regime, it is possible to define $E_\gamma^{\text{LI}} = \frac{m_e^2}{4\epsilon K(1-K)}$. The math can be simplified by the introduction of the dimensionless variables

$$x_\gamma = \frac{E_\gamma}{E_\gamma^{\text{LI}}}, \quad (2.5)$$

and

$$\Lambda_{\gamma,n} = \frac{E_\gamma^{\text{LI}(n+1)}}{4\epsilon} \delta_{\gamma,n}. \quad (2.6)$$

Then, equation 2.4 takes the form

$$\Lambda_{\gamma,n} x_\gamma^{n+2} + x_\gamma - 1 = 0. \quad (2.7)$$

Studying the values of $\delta_{\gamma,n}$ for which equation 2.7 has a solution, one can set the extreme allowed LIV coefficient [12, 25]. The limit LIV coefficient ($\delta_{\gamma,n}^{\text{lim}}$) for which the interaction is kinematically allowed for a given E_γ and ϵ is given by:

$$\delta_{\gamma,n}^{\text{lim}} = -4 \frac{\epsilon}{E_\gamma^{\text{LI}(n+1)}} \frac{(n+1)^{n+1}}{(n+2)^{n+2}}. \quad (2.8)$$

Figure 1 also shows $\delta_{\gamma,0}^{\text{lim}}$ as blue points. Equation 2.7 has real solutions for x_γ only if $\delta_{\gamma,n} > \delta_{\gamma,n}^{\text{lim}}$. Therefore, under the LIV model considered here, if $\delta_{\gamma,n} < \delta_{\gamma,n}^{\text{lim}}$, high energy photons would not interact with the background photons.

For a given E_γ and $\delta_{\gamma,n}$ the threshold background photon energy ($\epsilon_{th}^{\text{LIV}}$) including LIV effects is:

$$\epsilon_{th}^{\text{LIV}} = \frac{m_e^2}{4E_\gamma K(1-K)} - \frac{\delta_{\gamma,n} E_\gamma^{n+1}}{4}. \quad (2.9)$$

The superscript LIV is used from now on for emphasis. In the next sections, $\epsilon_{th}^{\text{LIV}}$ as given by equation 2.9 will be used for the calculations of the mean free path of the $\gamma\gamma_{CB} \rightarrow e^+e^-$ interaction. Figure 2 shows the allowed parameter space of E_γ and ϵ for different values of $\delta_{\gamma,0}$. The gray areas are cumulative from darker to lighter gray. Figure 2 illustrates how the mean free path is going to be affected by LIV effects given the dependence of the allowed pair production area on the LIV coefficients.

3 Photon horizon including LIV effects

The optical depth, $\tau_\gamma(E_\gamma, z)$, quantifies how opaque to photons the Universe is. The survival probability, i.e., the probability that a photon (γ) emitted with a given energy (E_γ) and at a given redshift (z) reaches Earth without interacting with the background, is given by:

$$P_{\gamma \rightarrow \gamma}(E_\gamma, z) = e^{-\tau_\gamma(E_\gamma, z)}. \quad (3.1)$$

The photon horizon is the distance (z_h) for which $\tau_\gamma(E_\gamma, z_h) = 1$. z_h defines, as a function of the energy of the photon, the distance over which a photon has probability $P_{\gamma \rightarrow \gamma} = 1/e$ of reaching Earth. The evaluation of the photon horizon is itself of extreme importance because it summarizes the visible Universe as a function of the energy of the emitted photon. In this section, the photon horizon is calculated including LIV effects. The argument presented in reference [10] is followed here.

In the intergalactic medium, the $\gamma\gamma_{CB} \rightarrow e^+e^-$ interaction is the main contribution to determine the photon horizon. In the approximation where cosmological effects are negligible, the mean free path ($\lambda(E_\gamma)$) of this interaction is given by:

$$\lambda(E_\gamma) = \frac{cz}{H_0\tau_\gamma(E_\gamma)}, \quad (3.2)$$

where $H_0 = 70 \text{ km s}^{-1} \text{ Mpc}^{-1}$ is the Hubble constant. The optical depth is obtained by:

$$\tau_\gamma = \int_0^z dz \frac{c}{H_0(1+z)\sqrt{\Omega_\Lambda + \Omega_M(1+z)^3}} \times \int_{-1}^1 d(\cos\theta) \frac{1 - \cos\theta}{2} \int_{\epsilon_{th}^{LIV}}^\infty d\epsilon n_\gamma(\epsilon, z) \sigma(E_\gamma, \epsilon, z), \quad (3.3)$$

where c is the speed of light in vacuum, θ the angle between the direction of propagation of both photons $\theta = [-\pi, +\pi]$, $\Omega_\Lambda = 0.7$ is the dark energy density, $\Omega_M = 0.3$ is the matter density and ϵ_{th}^{LIV} is the threshold energy of the interaction as given by equation 2.9.

$n_{\gamma_{CB}}$ is the background photon density. The dominant backgrounds are the Extragalactic Background Light (EBL) for $E_\gamma < 10^{14.5} \text{ eV}$, the Cosmic Background Microwave Radiation (CMB) for $10^{14.5} \text{ eV} < E_\gamma < 10^{19} \text{ eV}$ and the Radio Background (RB) for $E_\gamma > 10^{19} \text{ eV}$. In the calculations presented here, the Gilmore EBL model [16] was used. Since LIV effects in the photon horizon are expected only at the highest energies ($E_\gamma > 10^{16} \text{ eV}$) different models of EBL would give the same results. For the RB, the data from Gervasi et al. [15] with a cutoff at 1 MHz were used. Different cutoffs in the RB data lead to different photon horizons as shown in reference [10]. Since no new effect shows up in the LIV calculation due to the RB cutoff, only the 1 MHz cutoff will be presented.

σ is the cross-section of the interaction. No LIV effects are considered in the cross-section calculation. The Breit-Wheeler [5] cross-section was used:

$$\sigma(E, \epsilon, \theta) = \frac{2\pi\alpha^2}{3m_e^2} W(\beta), \quad (3.4)$$

with

$$W(\beta) = (1 - \beta^2) \times \left[2\beta(\beta^2 - 2) + (3 - \beta^2) \ln \left(\frac{1 + \beta}{1 - \beta} \right) \right], \quad (3.5)$$

where β refers to the speed of the electron-positron pair in the center-of-mass reference frame:

$$\beta(E, \epsilon, \theta) = \left(1 - \frac{2m_e^2 c^4}{E\epsilon(1 - \cos\theta)} \right)^{1/2}. \quad (3.6)$$

Figures 3, 4 and 5 show the mean free path for $\gamma\gamma_{CB} \rightarrow e^+e^-$ as a function of the energy of the photon (E_γ) for several LIV coefficients with $n = 0$, $n = 1$ and $n = 2$, respectively. The main effect is an increase in the mean free path that becomes stronger the larger the photon energy (E_γ) and the LIV coefficient are. Consequently, fewer interactions happen and the photon (γ) will have a higher probability of traveling further than it would have in a LI scenario. Similar effects due to LIV are seen for $n = 0$, $n = 1$ and $n = 2$. The LIV coefficients are treated as free parameters, therefore there is no way to compare the importance of the effect between the orders $n = 0$, $n = 1$ and $n = 2$, each order must be limited independently. Note that $\delta_{\gamma,n}$ units depend on n .

The LIV effect becomes more tangible in figure 6 in which the photon horizon (z_h) is shown as a function of E_γ . For energies above $E_\gamma > 10^{16.5}$ eV, the photon horizon increases when LIV is taken into account increasing the probability that a distant source emitting high energy photons produces a detectable flux at Earth.

4 GZK photons including LIV effects

UHECRs interact with the photon background producing pions (photo-pion production). Pions decay shortly after production generating EeV photons among other particles. The effect of this interaction chain suppresses the primary UHECR flux and generates a secondary flux of photons [14]. The effect was named GZK after the authors of the original papers [18, 36]. The EeV photons (GZK photons) also interact with the background photons as described in the previous sections. The study of GZK photons considering LIV is presented in this section.

In order to consider LIV in the GZK photon calculation the CRPropa3/Eleca [4, 31] programs were modified. The mean free paths calculated in section 3 were implemented in the CRPropa3/Eleca codes and the propagation of the particles was simulated. UHECR sources were homogeneously distributed in the Universe emitting protons with a power-law energy spectrum with index -2.7 and maximum energy of $E_{max} = 10^{21}$ eV. The UHECR flux reaching Earth was normalized to the flux measured by the Pierre Auger Observatory at $E = 10^{18.85}$ eV.

Figure 7 shows the integral flux of GZK photons obtained for $n = 0$ and some values of LIV coefficients. The black line ($\delta_{\gamma,0} = 0$) corresponds to the LI scenario. The flux is very sensitive to the LIV coefficients and increases with $\delta_{\gamma,n}$. One order of magnitude more GZK photons are expected for moderate values of the LIV coefficients ($\delta_{\gamma,0} = -10^{-21}$) when comparing with the LI predictions.

5 Conclusions

In this paper the effect of possible LIV in the propagation of photons in the Universe is studied. The interaction of a high energy photon traveling in the photon background was solved under LIV in the photon sector hypothesis. An innovative illustration of the solution was presented in section 2. The mean free path of the $\gamma\gamma_{CB} \rightarrow e^+e^-$ interaction was calculated considering LIV effects. Moderate LIV coefficients introduce a significant change in the mean free path of the interaction as shown in section 3 and figures 3, 4 and 5. The corresponding LIV photon horizon was calculated as shown in figure 6.

The effect of LIV in the flux of GZK photons was calculated in section 4 and is shown in figure 7. The flux of GZK photons reaching Earth increases significantly for small negative

values of the LIV coefficients ($\delta_{\gamma,n}$). An increase of the photon flux by more than one order of magnitude for $\delta_{\gamma,0} = -10^{-21}$ was calculated. The upper limits in the photon flux measured by the UHECR experiments [7, 17] can be used to set limits on the LIV coefficients and therefore on the possible Lorentz Invariance Violation.

Acknowledgments

RGL is supported by FAPESP (2014/26816-0).HMH acknowledges IFSC/USP for their hospitality during the developments of this work, Abdel Pérez Lorenzana for enlightening discussions and the support from Conacyt Mexico under grant 237004. VdS thanks the Brazilian population support via FAPESP (2015/15897-1) and CNPq. This work has partially made use of the computing facilities of the Laboratory of Astroinformatics (IAG/USP, NAT/Unicsul), whose purchase was made possible by the Brazilian agency FAPESP (2009/54006-4) and the INCT-A.

References

- [1] A. Abramowski et al. Search for Lorentz invariance breaking with a likelihood fit of the PKS 2155-304 flare data taken on MJD 53944. *Astropart. Phys.*, 34:738–747, 2011.
- [2] G. Amelino-Camelia, John R. Ellis, N. E. Mavromatos, Dimitri V. Nanopoulos, and Subir Sarkar. Tests of quantum gravity from observations of gamma-ray bursts. *Nature*, 393:763–765, 1998.
- [3] W. B. Atwood et al. The large area telescope on the Fermi gamma-ray space telescope mission. *The Astrophysical Journal*, 697(2):1071, 2009.
- [4] Rafael Alves Batista, Andrej Dundovic, Martin Erdmann, Karl-Heinz Kampert, Daniel Kuempel, Gero Mller, Guenter Sigl, Arjen van Vliet, David Walz, and Tobias Winchen. CRPropa 3 - a public astrophysical simulation framework for propagating extraterrestrial ultra-high energy particles. *JCAP*, 2016(05):038, 2016.
- [5] G. Breit and John A. Wheeler. Collision of two light quanta. *Phys. Rev.*, 46:1087–1091, Dec 1934.
- [6] Sidney Coleman and Sheldon L. Glashow. High-energy tests of Lorentz invariance. *Phys. Rev. D*, 59:116008, 1999.
- [7] Telescope Array Collaboration. Upper limit on the flux of photons with energies above 10^{19} eV using the Telescope Array surface detector. *Phys. Rev. D*, 88:112005, Dec 2013.
- [8] The Pierre Auger Collaboration. The Pierre Auger Cosmic Ray Observatory. *Nuclear Instruments and Methods in Physics Research Section A: Accelerators, Spectrometers, Detectors and Associated Equipment*, 798:172 – 213, 2015.
- [9] The CTA Consortium. Design concepts for the Cherenkov Telescope Array CTA: an advanced facility for ground-based high-energy gamma-ray astronomy. *Experimental Astronomy*, 32(3):193–316, 2011.
- [10] A. De Angelis, G. Galanti, and M. Roncadelli. Transparency of the universe to gamma-rays. *Monthly Notices of the Royal Astronomical Society*, 2013.
- [11] Benjamin Zitzer for the VERITAS Collaboration. Lorentz invariance violation limits from the crab pulsar using VERITAS. *Braz.J.Phys.*, 44:4, 2014.
- [12] Matteo Galaverni and Gunter Sigl. Lorentz Violation and Ultrahigh-Energy Photons. *Phys. Rev.*, D78:063003, 2008.

- [13] Matteo Galaverni and Gunter Sigl. Lorentz Violation in the Photon Sector and Ultra-High Energy Cosmic Rays. *Phys. Rev. Lett.*, 100:021102, 2008.
- [14] Graciela Gelmini, Oleg Kalashev, and Dmitry V. Semikoz. GZK photons in the minimal ultra-high energy cosmic rays model. *Astroparticle Physics*, 28(45):390 – 396, 2007.
- [15] M. Gervasi, A. Tartari, M. Zannoni, G. Boella, and G. Sironi. The contribution of the unresolved extragalactic radio sources to the brightness temperature of the sky. *The Astrophysical Journal*, 682(1):223, 2008.
- [16] R. Gilmore and E. Ramirez-Ruiz. Local absorption of high-energy emission from gamma-ray bursts. *The Astrophysical Journal*, 721(1):709, 2010.
- [17] A. V. Glushkov, I. T. Makarov, M. I. Pravdin, I. E. Sleptsov, D. S. Gorbunov, G. I. Rubtsov, and S. V. Troitsky. Constraints on the flux of primary cosmic-ray photons at energies $E > 10^{18}$ eV from Yakutsk muon data. *Phys. Rev. D*, 82:041101, Aug 2010.
- [18] Kenneth Greisen. End to the Cosmic-Ray spectrum? *Phys. Rev. Lett.*, 16(17):748, April 1966.
- [19] Andreas Haungs, Gustavo Medina-Tanco, and Andrea Santangelo. Special issue on the JEM-EUSO mission. *Experimental Astronomy*, 40(1):1–2, 2015.
- [20] T. Jacobson, S. Liberati, and D. Mattingly. Threshold effects and Planck scale Lorentz violation: Combined constraints from high-energy astrophysics. *Phys. Rev.*, D67:124011, 2003.
- [21] F. R. Klinkhamer and M. Schreck. New two-sided bound on the isotropic Lorentz-violating parameter of modified-Maxwell theory. *Phys. Rev.*, D78:085026, 2008.
- [22] S. Liberati and L. Maccione. Quantum Gravity phenomenology: achievements and challenges. *J. Phys. Conf. Ser.*, 314:012007, 2011.
- [23] Stefano Liberati and Luca Maccione. Lorentz violation: Motivation and new constraints. *Annual Review of Nuclear and Particle Science*, 59(1):245–267, November 2009.
- [24] Luca Maccione and Stefano Liberati. GZK photon constraints on Planck scale Lorentz violation in QED. *JCAP*, 0808:027, 2008.
- [25] H. Martínez-Huerta and A. Pérez-Lorezana. Restrictive scenarios from Lorentz Invariance Violation to cosmic rays propagation. 2016. arXiv 1610.00047.
- [26] David Mattingly. Modern tests of Lorentz invariance. *Living Reviews in Relativity*, 8, 2005.
- [27] J. Holder for the VERITAS Collaboration. *Proc. International Cosmic Ray Conference*, 12, 2011.
- [28] The HESS Collaboration. Observations of the crab nebula with hess. *Astronomy and Astrophysics*, 457(3):899–915, 2006.
- [29] The MAGIC Collaboration. The major upgrade of the MAGIC telescopes, Part I: The hardware improvements and the commissioning of the system. *Astroparticle Physics*, 72:61 – 75, 2016.
- [30] Robert C. Myers and Maxim Pospelov. Ultraviolet modifications of dispersion relations in effective field theory. *Phys. Rev. Lett.*, 90:211601, 2003.
- [31] Mariangela Settimo and Manlio De Domenico. Propagation of extragalactic photons at ultra-high energy with the EleCa code. *Astroparticle Physics*, 62:92 – 99, 2015.
- [32] Floyd W. Stecker and S. T. Scully. Lorentz invariance violation and the spectrum and source power of ultrahigh energy cosmic rays. *Astropart. Phys.*, 23:203–209, 2005.
- [33] Floyd W. Stecker and Sean T. Scully. Searching for New Physics with Ultrahigh Energy Cosmic Rays. *New J. Phys.*, 11:085003, 2009.

- [34] Peter Tinyakov. Latest results from the Telescope Array. *Nuclear Instruments and Methods in Physics Research Section A: Accelerators, Spectrometers, Detectors and Associated Equipment*, 742:29 – 34, 2014. 4th Roma International Conference on Astroparticle Physics.
- [35] V. Vasileiou, A. Jacholkowska, F. Piron, J. Bolmont, C. Couturier, J. Granot, F. W. Stecker, J. Cohen-Tanugi, and F. Longo. Constraints on Lorentz invariance violation from Fermi-Large area telescope observations of gamma-ray bursts. *Phys. Rev. D*, 87:122001, 2013.
- [36] G. T. Zatsepin and V. A. Kuz'min. *ZhETF Pis'ma*, 4:114, 1966.
- [37] Benjamin Zitzer. Lorentz Invariance Violation Limits from the Crab Pulsar using VERITAS. In *Proceedings, 33rd International Cosmic Ray Conference (ICRC2013): Rio de Janeiro, Brazil, July 2-9, 2013*, page 1147, 2013.

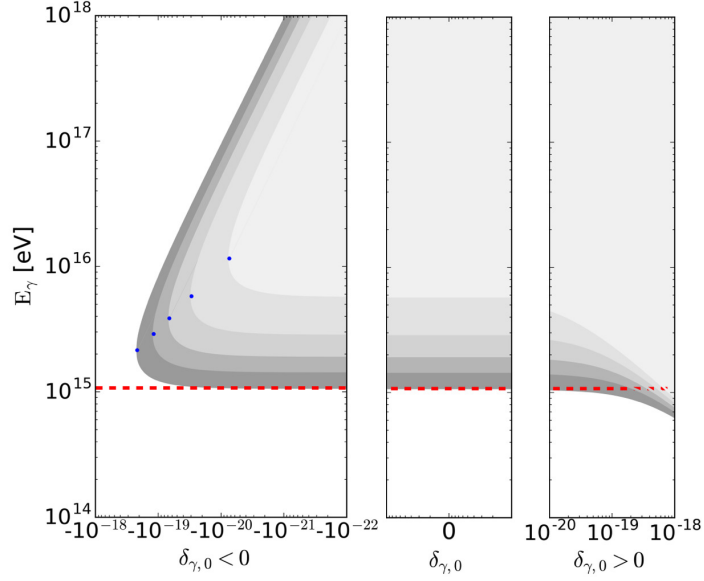


Figure 1. Allowed regions of the high energy photon (E_γ) and $\delta_{\gamma,0}$ for the $\gamma\gamma_{CB} \rightarrow e^+e^-$ interaction considering LIV effects. Gray regions show for each case the space parameter for which equation 2.4 is solvable. The left panel corresponds to $\delta_{\gamma,0} < 0$, the center panel corresponds to the LI solution with $\delta_{\gamma,0} = 0$ and the right panel to the solutions with $\delta_{\gamma,0} > 0$. Four cases of the background photon energy (ϵ) are shown corresponding to temperatures of 2.7, 2, 1.5 and 1 K, from dark to light gray, respectively. The red dashed line is a reference for $\delta_{\gamma,0} = 0$ (LI case) with ϵ corresponding to 2.7 K. The blue points represents $\delta_{\gamma,0}^{lim}$ as calculated in equation 2.8.

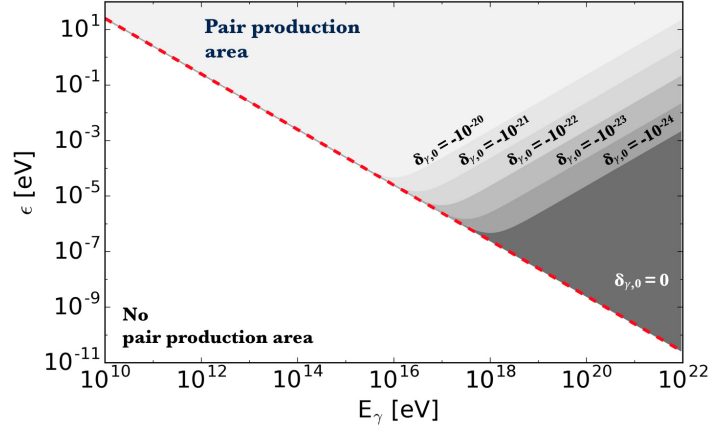


Figure 2. Allowed regions for the pair production in the $\gamma\gamma_{CB} \rightarrow e^+e^-$ interaction considering LIV effects. The high energy photon (E_γ) and background photon (ϵ) parameter space is shown divided in gray regions for each value of $\delta_{\gamma,0}$. The gray areas are cumulative from darker to lighter gray. The red dashed line is a reference for $\delta_{\gamma,0} = 0$ (LI case).

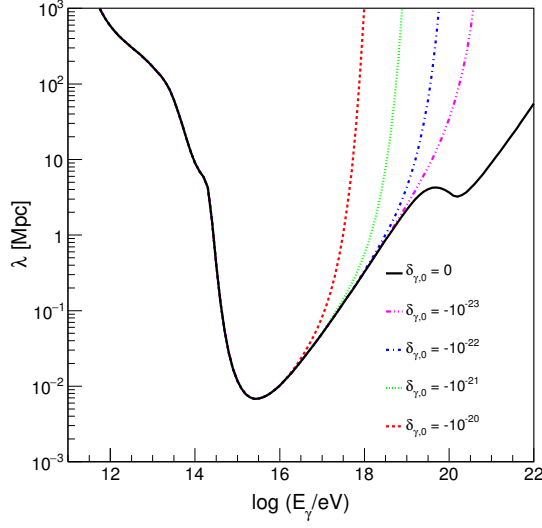


Figure 3. Mean free path (λ) for $\gamma\gamma_{CB} \rightarrow e^+e^-$ as a function of the energy of the photon (E_γ) shown for several LIV coefficients for $n = 0$. The Gilmore model [16] for EBL and Gervasi et al. [15] model for the RB with a cutoff at 1 MHz were used. The black continuous line is the LI scenario. The colored lines are different values for the LIV coefficients. The colored lines coincide with the black line for $\log(E_\gamma/\text{eV}) < 15$.

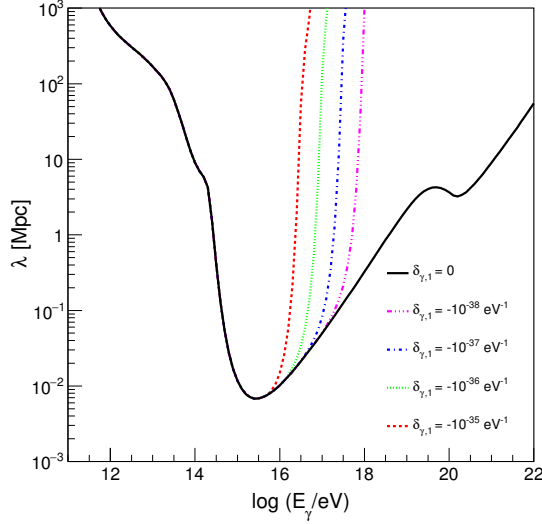


Figure 4. Mean free path (λ) for $\gamma\gamma_{CB} \rightarrow e^+e^-$ as a function of the energy of the photon (E_γ) shown for several LIV coefficients for $n = 1$. The Gilmore model [16] for EBL and Gervasi et al. [15] model for the RB with a cutoff at 1 MHz were used. The black continuous line is the LI scenario. The colored lines are different values for the LIV coefficients. The colored lines coincide with the black line for $\log(E_\gamma/\text{eV}) < 15$.

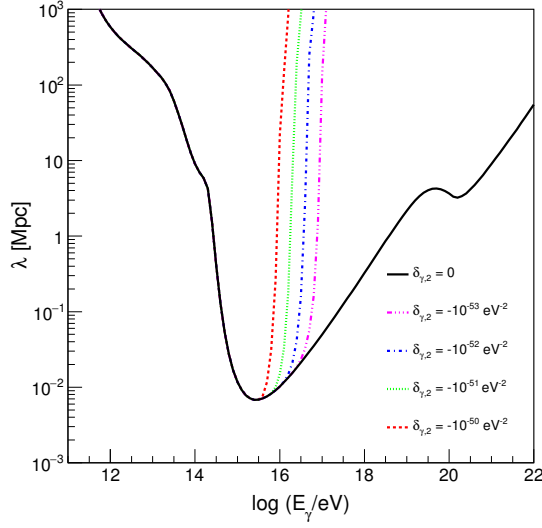


Figure 5. Mean free path (λ) for $\gamma\gamma_{CB} \rightarrow e^+e^-$ as a function of the energy of the photon (E_γ) shown for several LIV coefficients for $n = 2$. The Gilmore model [16] for EBL and Gervasi et al. [15] model for the RB with a cutoff at 1 MHz were used. The black continuous line is the LI scenario. The colored lines are different values for the LIV coefficients. The colored lines coincide with the black line for $\log(E_\gamma/eV) < 15$.

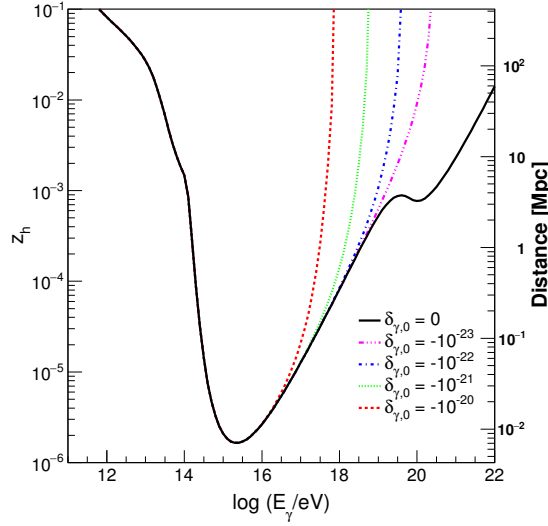


Figure 6. Photon horizon (z_h) as a function of the photon energy (E_γ) for different LIV coefficients with $n = 0$. The right axis shows the equivalent distance obtained using the same assumptions used in equation 3.3. The Gilmore model [16] for EBL and Gervasi et al. [15] model for the RB with a cutoff at 1 MHz were used. The black continuous line represents the LI scenario. The colored lines are different values for the LIV coefficients. The colored lines coincide with the black line for $\log(E_\gamma/eV) < 15$.

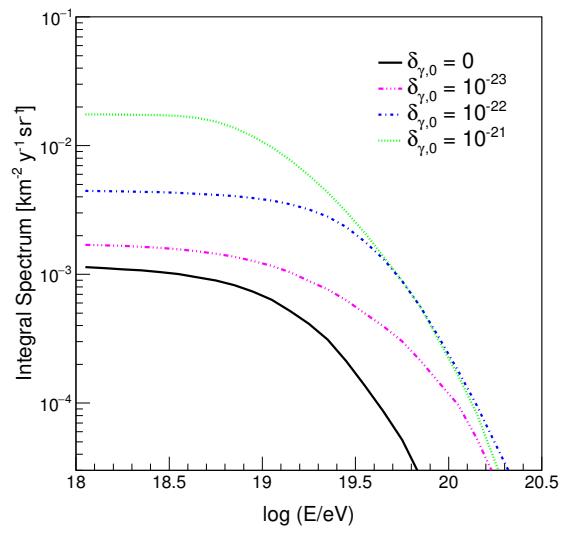


Figure 7. Integral of the energy spectrum of GZK photons reaching Earth as a function of the photon energy (E_γ) considering LIV effects for $n = 0$. The black continuous line represents the LI scenario. The colored lines are different values for the LIV coefficients.